PAPER

Immobilized Pd-Ag bimetallic nanoparticles on polymeric nanofibers as an effective catalyst: effective loading of Ag with bimetallic functionality through Pd nucleated nanofibers

View the article online for updates and enhancements.

Immobilized Pd-Ag bimetallic nanoparticles on polymeric nanofibers as an effective catalyst: effective loading of Ag with bimetallic functionality through Pd nucleated nanofibers

Kugalur Shanmugam Ranjith[1], Asli Celebioglu and Tamer Uyar[1] ![ORCID]

Institute of Materials Science & Nanotechnology and UNAM–National Nanotechnology Research Center, Bilkent University, Ankara, 06800, Turkey

E-mail: tamer@unam.bilkent.edu.tr and ranjuphy@gmail.com

Abstract

Here, we present a precise process for synthesizing Pd-Ag bimetallic nanoparticles (NPs) onto polymeric nanofibers by decorating Pd-NPs through atomic layer deposition followed by a chemical reduction process for tagging Ag nanostructures with bimetallic functionality. The results show that Pd-NPs act as a nucleation platform for tagging Ag and form Pd-Ag bimetallic NPs with a monodisperse nature with significant catalytic enhancement to the reaction rate over the bimetallic nature of the Pd-Ag ratio. A Pd-NP decorated polymeric nanofibrous web acts as an excellent platform for the encapsulation or interaction of Ag, which prevents agglomeration and promotes the interaction of Ag ions only on the surface of the Pd-NPs. We observed an effective reduction of 4-nitrophenol (4-NP) to 4-aminophenol (4-AP) by sodium borohydride (NaBH$_4$) to access the catalytic activity of Pd-Ag bimetallic NPs on a free-standing flexible polymeric nanofibrous web as a support. The captive formation of the polymeric nanofibrous web with Pd-Ag bimetallic functionality exhibited superior and stable catalytic performance with reduction rates of 0.0719, 0.1520, and 0.0871 min^{-1} for different loadings of Ag on Pd decorated nanofibrous webs such as Pd/Ag(0.01), Pd/Ag(0.03), and Pd/Ag(0.05), respectively. The highly faceted Pd-Ag NPs with an immobilized nature improves the catalytic functionality by enhancing the binding energy of the 4-NP adsorbate to the surface of the NPs. With the aid of bimetallic functionality, the nanofibrous web was demonstrated as a hybrid heterogeneous photocatalyst with a 3.16-fold enhancement in the reaction rate as compared with the monometallic decorative nature of NaBH$_4$ as a reducing agent. The effective role of the monodisperse nature of Pd ions with an ultralow content as low as 3 wt% and the tunable ratio of Ag on the nanofibrous web induced effective catalytic activity over multiple cycles.

Supplementary material for this article is available online

Keywords: atomic layer deposition (ALD), bimetallic nanoparticles, Pd-Ag nanoparticles, nanofibers, catalysis

(Some figures may appear in colour only in the online journal)

[1] Authors to whom any correspondence should be addressed.

Introduction

The interest in the bimetallic form of nanostructures has expanded to their application as an efficient catalyst with significant properties which arise at the heterostructural interface. Following previous catalyst based research, Pd based nanocatalysts have been known to exhibit excellent catalytic activity towards reaction systems such as aerobic oxidation of alcohols [1–3], synthesizing polysubstituted olefins [4], nitrite reduction [5], CO oxidative coupling reactions [6], stille coupling reactions [7], and so on. Control over the morphology, size, and alloying nature with other nanostructures, Pd based catalysts have exhibited effective properties by avoiding the disadvantages such as lower sensitivity and lower efficiency [8, 9]. Metal catalysts with different morphologies have played a crucial role in the arrangement of atoms and dominate certain strategies that can improve the catalytic activity. Further, catalytic nanostructures with a size around 2–5 nm are considered to be an optimal size which exhibit higher efficiency catalytic performance [10]. The arrangement of high index facets of the nanocatalyst exhibits faster catalytic performance than the regular facets that contradict the expression of high density of steps and ledges that lead to the promotion of active sites for breaking the chemical bonds [11]. The Pd based bimetallic forms of nanostructures such as Pd-Ni, Pd-Cu, Pd-Pt, Pd-Au, and Pd-Ag play an extensive role in chemical reactions such as reduction of oxygen [12], CO_2 hydration [13], CO reduction [14, 15], hydration of nitrophenol (4-NP) [16, 17], dry reforming reaction [18], and dechlorination process [19]. The reduction of industrial pollutants such as 4-NP with the accomplishment of reaction in the presence of the metal catalyst is of interest in a hybrid platform [20]. Moreover, bimetallic catalysts endowed with Pd ions demonstrate much more stability over the poisoning effect and result in better catalytic activity than their single counter parts.

Inherently, Ag is one of the two transition metals that are more electronegative than Pd. So, incorporating Ag with Pd results in a unique effect on the nanostructural surfaces that facilitate the catalytic reaction. In early investigations, the high catalytic behavior of Pd-Ag bimetallic nanostructures was observed in the hydration of nitrophenol to aminophenol [18] and in the oxidation of methanol [21]. The improvement in the catalytic properties were due to the effective substitution of Pd with Ag ions which revealed a mixed phase with twin defective surfaces with an improved electronic effect through its bimetallic nature. However, the ratio between Pd and Ag plays a crucial role because of the lower catalytic activity of Ag as compared with Pd which influences a higher Ag concentration. By understanding the functionality, Pd-Ag bimetallic nanostructures can be used in interesting applications such as hydrogenation and oxidization reactions. But the miscibility gap between Pd and Ag creates a challenge in synthesizing the Pd-Ag bimetallic form of nanoparticles (NPs). Further, designing the catalyst based support is a crucial step that challenges the formation of bimetallic nanostructures in order to avoid the aggregation of metal nanostructures under harsh reaction conditions specifically in organic solutions which results in a reduction of the catalytic activity [22]. A strategy used to prevent the agglomeration is to immobilize the metal nanostructures on a support or substrate, such as a silica substrate, glass substrate, carbon nanofibers, and polymer nanowebs, which delivers improved performance but faces complexity in the synthesis process [23–26].

Decorating metal nanostructures over the electrospun polymeric nanofibers facilitates the reaction process as well as enables the formation of bimetallic NPs with some stability during the catalytic reduction. Difficulties over the uniform loading of metal nanostructures on the nanofiber based support during the chemical reduction process has initiated the investigation of the physical form of the interaction of metal NPs on the nanofibers to design a hybrid web form of substrate. Atomic layer deposition (ALD) is one of the promising methods to control the metal interaction at the atomic level with self-limited surface interactions [27] which facilitates the interaction of mono-dispersed Pd-NPs on a polymeric nanofibrous web [28]. Due to the self-limiting process, the loading ratio of the catalyst is controlled on the supportive substrate with the maximized surface interaction of the catalyst [29]. Higher surface area and the favorable chemical interaction on the nanofiber surface initiate the decoration of Pd-NPs with uniform loading and decoration through the ALD process. More importantly, the nanofiber network selectively favors the interaction of Pd-NPs only with the Ag ions in the reduction process, through the poor interaction of Ag on the polymeric surface depending on its surface functionality. Additionally, a supportive nanofibrous web promotes the interaction of the catalyst with high stability and recoverability after multiple catalytic reactions. Further, it contributes to avoiding the agglomeration of the catalyst during the chemical reactions, and controlling the immobilized nature of the catalyst in the supportive web. There are previous reports on Pd-Ag based bimetallic nanostructures [30] but constructing the heterostructure platform over the nanofiber based support increases the interest in the catalytic reaction due to the higher surface area of the catalyst to promote the catalytic reaction.

Herein, Pd-NPs were decorated over electrospun polymeric (i.e. nylon) nanofibers through the ALD technique followed by the wet chemical reduction strategy to fabricate the Pd-Ag bimetallic NPs over the nanofiber network with different Pd:Ag ratios. The catalytic performance over the resultant bimetallic support was assessed by studying the catalytic reduction of 4-nitrophenol (4-NP) to aminophenol (4-AP) with different Pd:Ag ratios, different dosages, and in different temperatures. The prepared bimetallic NPs offer better catalytic activity in terms of stability after multiple cycles with respect to monometallic Pd and Ag nanostructures and compared with the commercially available catalysts.

Experimental process

Materials

Nylon 6,6 (Mw 230.000-280.000, Scientific Polymer Products, Inc), palladium(II) hexafluoroacetylacetonate (Pd(hfac)$_2$, Strem Chemicals), formalin (HCOH, Sigma-Aldrich), N,N- dimethylformamide (DMF, Pestanal, Riedel), formic acid (HCOOH, 98%, Sigma-Aldrich), silver nitrate (AgNO$_3$, Sigma-Aldrich), 4-nitrophenol (4-NP, 99%, Alfa Aesar), methanol (CH$_3$OH, Sigma-Aldrich), sodium borohydride (NaBH$_4$, fine granular, Merck) were obtained commercially. All materials were used without any purification. De-ionized (DI) water was obtained using a Millipore Milli-Q system.

Electrospinning of nylon nanofibrous webs

A bead-free uniform homogeneous nylon nanofibrous web was prepared from the clear solutions of 8% Nylon 6,6 in formic acid through the electrospinning process [31]. First, we prepared the nylon: a formic acid homogeneous solution was loaded into a 10 ml syringe fitted with a metallic needle with a 0.4 mm inner diameter. The syringe was loaded on the syringe pump (KD Scientific, KDS 101) with a 1 ml h^{-1} flow rate and at high voltage; 10 kV was applied with a high voltage power supply (Matsusada, AU Series) to the tip of the needle. Inducing the higher voltage at the needle tip initiated the electrospinning jet movement through the aluminum foil covered stationary plate metal collector which was placed 10 cm from the end of the tip. The electrospinning process was carried out at ∼25 °C and 22% relative humidity in an enclosed Plexi-glass chamber. The collected nanofibrous web was placed in the hood overnight to remove any residual solvent present.

Surface decoration of Pd-NPs on a nylon nanofibrous web by ALD

A monodispersive form of Pd-NPs was decorated on the free-standing electrospun nylon nanofibrous webs through the ALD process [28]. Through the exposed mood using Pd(hfac)$_2$ as the Pd precursor and formalin (HCOH, 30% in aqueous solution with 15% methanol) as counter reactants, Pd-NPs were directly decorated on the polymeric nanofiber surface. The precursor temperature was set at 70 °C to attain the vapor pressure and the substrate temperature was set at 200 °C for the uniform deposition of the Pd-NPs throughout the nanofibrous web. N$_2$ was used as the carrier gas at a flow rate of 20 sccm under a dynamic vacuum condition. Fifteen cycles were deposited for the decoration of the Pd-NPs.

Surface decoration of Ag ions on a Pd decorated nylon nanofibrous web

Chemical reduction was carried out on free-standing Pd decorated nylon nanofibrous webs for decorating the Ag with Pd-NPs on the surface of nanofibers. The Pd decorated nylon nanofibrous webs were immersed in an aqueous solution of NaBH$_4$ (0.05 mol), and a homogeneous aqueous solution of AgNO$_3$ (0.01–0.05 mM) was added dropwise while under continuous stirring at room temperature. After completely mixing the NaBH$_4$ with AgNO$_3$, the solution was heated to 60 °C and the temperature was maintained for 6 h. The immersed webs were collected and cleaned in distilled water and dried under vacuum for 3 h. Depending on the AgNO$_3$ concentration (0.01, 0.03, and 0.05 mM), the catalytic fibrous web samples were named Pd/Ag(0.01)-Nylon, Pd/Ag(0.03)-Nylon, and Pd/Ag(0.05)-Nylon, respectively.

Characterizations

The nanofibrous morphology of the pristine electrospun nylon nanofibrous web and Pd and Pd-Ag decorated nylon nanofibrous webs were investigated using a scanning electron microscope (SEM, FEI–Quanta 200 FEG). For clear imaging, 5 nm of Ag-Pd was coated on the nanowebs during the SEM measurements. Transmission electron microscope (TEM, FEI–Tecnai G2F30, Hillsboro, OR, USA) evidenced the detailed investigation of the formation of Pd decorated (Pd-Nylon) and Pd-Ag bimetallic NPs decorated nylon (Pd/Ag-Nylon) nanofibers. For preparing the sample for the TEM investigation, small pieces of metal NP decorated webs were sonicated in ethanol for 5 min to get the nanofiber dispersed solvent, followed by the dropping of suspension onto the copper TEM grids (HC200), and allowing them to dry under an IR lamp for a few minutes to remove the solvent. Through scanning transmission electron microscopy (STEM) the image recorded with energy dispersive x-ray spectroscopy (EDX) revealed the elemental mapping analysis. Through the PANalytical X'Pert Multi-Purpose x-ray Diffractometer with a Cu Kα radiation source ($\lambda = 0.154\,06$ nm) the powder x-ray diffraction (XRD) patterns were recorded for the metal decorated polymeric nanofibrous web. A Thermo Fisher Scientific spectrometer with an Al Kα x-ray source was equipped to analyze the x-ray photoelectron spectroscopy (XPS) measurements to detect the surface elemental composition of the pristine, Pd and Pd-Ag NPs decorated polymeric nanofibrous webs. Pd 3d and Ag 3d high resolution XPS scans were also taken at a pass energy of 30 eV, with energy steps of 0.1 eV in order to analyze the bonding states. The bulk compositions were analyzed using a Thermo, X series II inductively coupled plasma mass spectroscopy (ICP-MS) and for the measurements, the metal decorated polymeric nanofibers were dissolved at a 1:1 ratio of nitric acid:hydrochloric acid and compared with known standards with different concentrations (250, 125, 62.5, 32.25, and 16.125 ppb) for quantifying the presence of Pd and Ag in the polymeric nanofibrous web. Finally, the reusability performance of the Pd/Ag-Nylon nanofibrous web was checked by applying a slight washing step to the nanofibrous web in water after each catalyst reaction, and then the nanowebs are dried and used for the next cycles. After the reusability test, the morphology of the nanofibrous web was imaged by the SEM technique.
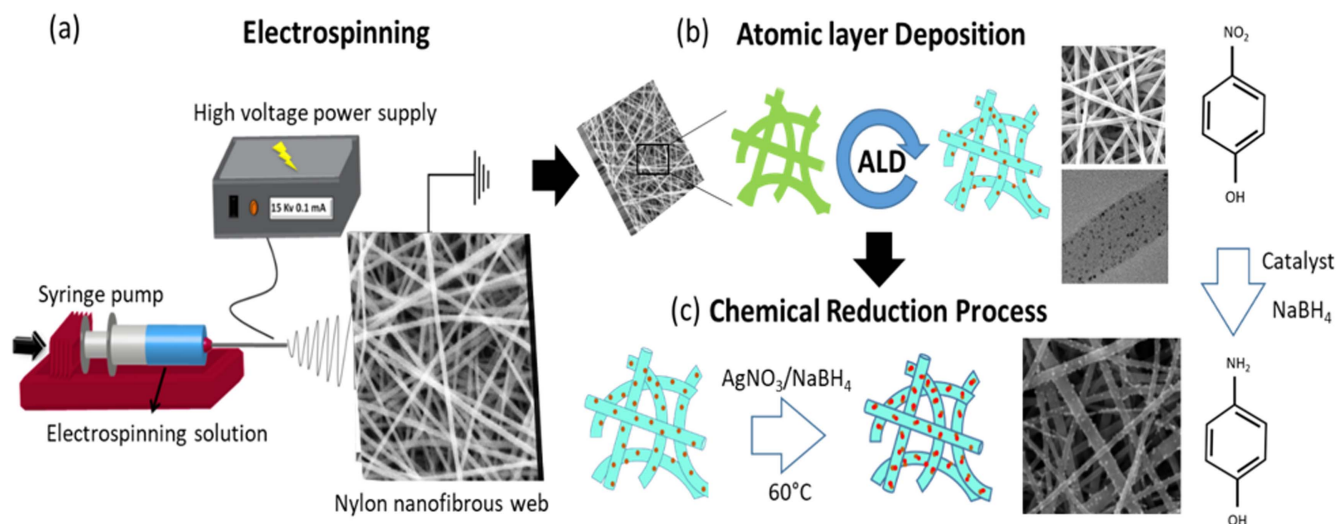
Figure 1. Schematic representations of the processing steps ((a) electrospinning followed by (b) ALD followed by (c) chemical reduction process) for the fabrication of the surface decorated bimetallic nanostructures (Pd-Ag-NPs) onto electrospun polymeric nanofibers for catalytic application.

Results and discussion

Figure 1 shows a schematic illustration of the formation of the Pd-Ag decorated electrospun nylon nanofibrous web through ALD followed by the chemical reduction process. Figure 2 shows the surface morphology of the electrospun nylon nanofibers as the function of Pd-Ag bimetallic nanostructure decoration through the SEM images. The electrospun nylon nanofiber had an average diameter of 60 nm (figures 2(a) and (b)) which was used as the support/substrate for the decoration of the Pd nanostructures through the ALD process. During the Pd deposition, nitrogen was used as a carrier gas in the reactive environment which ensured the interaction with the nylon nanofibers. After the decoration of the Pd-NPs, Ag based bimetallic functionality was formed through the chemical reduction process where the Pd acted as the nucleation platform for the decoration or loading of the Ag-NPs. The loading of the Ag concentration was tuned by varying the concentration of $AgNO_3$ in the reduction process and the effect of the Ag ratio with Pd on the nylon nanofibrous web was investigated for the hydrogenation based catalytic process. Figure 2 illustrates the morphological transformation of the nylon nanofiber during the ALD and chemical reduction process by the loading of metal ions. Figures 2(c) and (d) show the SEM images of 15 cycles of Pd decorated nylon nanofibers which reveal the absence of notable surface modification. But the color of the nanofibrous web had changed to gray (figure S1 is available online at stacks.iop.org/NANO/29/245602/mmedia) which reveals the surface interaction of the nanofibrous web during the ALD process.

After the Pd decoration through ALD, the Ag-NPs were decorated on the nanofibers through the chemical reduction process. While using 0.03 mM of $AgNO_3$ concentration in the reduction process, the resultant nanofibers appeared with the decoration of Ag ions with sizes of 4–10 nm throughout the nanofibrous web (figures 2(e) and (f)). Upon varying the concentration of $AgNO_3$ in the reduction process, the size of

the decorated Ag-NPs got larger with uniform distribution (figure S2). Upon increasing the concentration of the Ag ions in the reduction process, the particle size increased which is represented by a histogram (figure S2). In order to investigate the sole decorative effect of Ag ions on nylon nanofibers, similar chemical reduction processes were induced on the pristine nylon nanofibers (without Pd decoration through ALD). Figures 2(g) and (h) show the SEM images of the (0.03 mM) Ag-NP decorated nylon nanofibers, which reveals the lower presence of Ag ions on the nylon nanofibers as compared with the Pd decorated nylon nanofibers and the Ag-NPs were not uniformly distributed throughout the nanofibrous network. Further they did not chemically interact with the polymeric surface which was observed in the TEM investigation in the following part. This observation reveals that the Pd-NPs play a key role as nuclei for the loading or interaction of Ag ions on the nylon nanofibers. Further, Ag ions were decorated or grown promptly on the Pd lattice and not on the nylon surface. This indicates that Ag was decorated or interacted on the surface of the Pd-NPs during the reduction process and further grew, while Pd was oxidized [32]. The interactive feature of Pd and Ag produces the bimetallic form of nanostructures and the ratio of the Pd-Ag was identified from TEM-EDS (figure S3), and ICP-MS and XPS (table S1). The investigation of the bimetallic nature of Pd-Ag loaded nylon nanofibers was performed by TEM and HRTEM analysis, as shown in figures 3 and 4.

Figure 3(a) show the TEM images of nylon nanofiber induced in 15 cycles of Pd deposition. After the topical deposition, nearly 2 nm of Pd grains were decorated on the surface of the nylon nanofiber [28]. The lattice fringes represent the (111) phase of the Pd which was decorated throughout the nanofiber surface with a monodispersed assembly (figure 3(b)). However, while decorating the Ag ions directly onto the nylon surface without Pd-NPs, the Ag metal ions did not physically interact with the nanofiber surface during the chemical reaction (figures 3(c) and (d)).
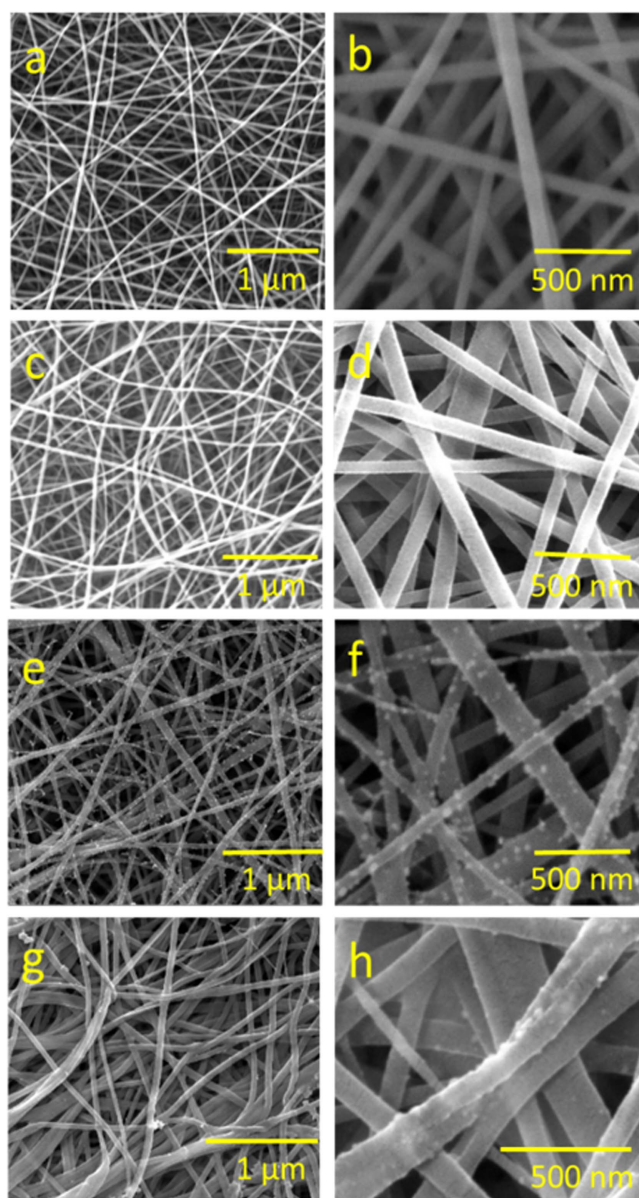
Figure 2. SEM and high magnified SEM images of (a), and (b) pristine nylon, (c) and (d) Pd-Nylon, (e) and (f) Pd/Ag(0.03)-Nylon, and (g) and (h) Ag (0.03)-Nylon nanofibrous webs.

Therefore, Ag did not obviously or stably interact on the nylon nanofiber surface (figures 3(c) and (d)) during the sample preparation process. This signifies the poor interaction of Ag ions with the nylon nanofiber surface. While inducing the Pd loaded nylon nanofiber for the decoration of Ag ions through the chemical reduction, it revealed the good interaction and loading of Ag ions on the nylon nanofibers (figures 4(a) and (b)). The HRTEM image (figures 4(c) and (d)) reveals the interesting phenomena that the Ag ions were loaded or interacted only on the Pd-NPs, not on the nylon surface which forms the Pd-Ag bimetallic phase. The average particle size of around ∼4 nm was decorated on the nylon nanofiber where the Pd-NPs were loaded. The chemically reduced Ag ions exhibit the phase orientation of a face center cubic (fcc) system with a size of
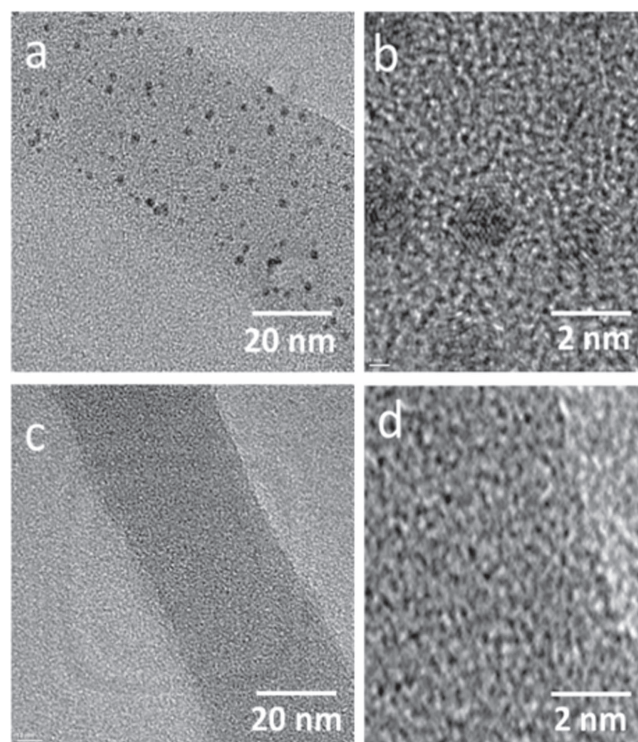

Figure 3. TEM and HRTEM images of metal decorated nylon nanofiber (a) and (b) Pd-Nylon through ALD process, (c) and (d) Ag-Nylon through chemical reduction process.

nearly 5 nm of coverage with Pd-NPs (figure 4(d)). On the nanofiber surface Pd sufficed as the nucleation site for the Ag metal ions to form the Pd-Ag bimetallic nanoparticles and the interactive nature of the Pd sites avoided the apparent aggregation favored by the inter-particle attraction between the Pd and Ag. The HRTEM images of the individual Pd-Ag-NPs reveal two sets of lattice fringes with interplanar spacings of 0.238 nm and 0.225 nm which represent the (111) fcc plane of the Ag and Pd ions, respectively [33, 34]. The result signifies the bimetallic phase of Pd-Ag-NPs with combined counter phases and the size distribution were nearly homogeneous with the narrow distribution on the surface. The appearance of the lattice fringes of the Pd as well as the Ag-NPs signifies crystallinity with an fcc structure. The HAADF-STEM-EDS mapping analysis of the Pd-Ag bimetallic NP decorated nanofiber surface conforms the conclusive distributed bimetallic nature of Pd-Ag-NPs (figures 4(e)–(h)). The overlapping of Ag-NPs on the Pd surface reveals uniform distribution throughout the nanofiber surface and indicate the formation of a Pd-Ag bimetallic nature. The EDS analysis indicates the average composition of 1:3 of Pd:Ag, which augments the ICP-MS results.

With increasing the Ag precursor concentration, to vary the ratio of Pd:Ag (Pd/Ag(0.01)-Nylon–Pd/Ag(0.05)-Nylon) the size distribution and the Ag concentration increased on the bimetallic surface (table S1; figure S4). A linear increase in the size distribution of the Ag-NPs is observed in the lower precursor concentration (0.01–0.03 mM). Ag loading on the nanofibrous web increased from 3%–30% with increasing the
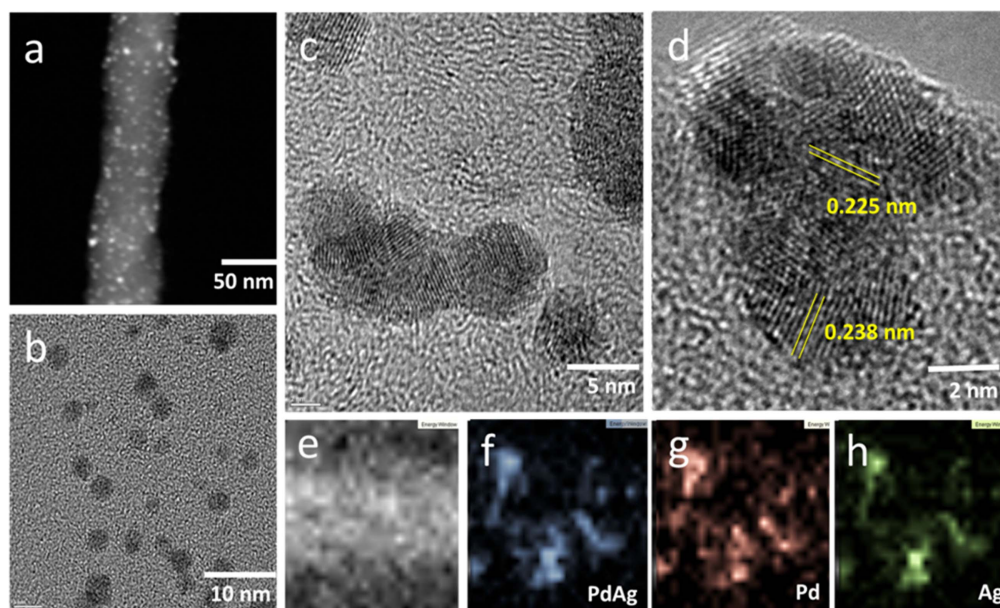
Figure 4. (a) STEM images of Pd-Ag-NPs decorated on nylon nanofiber, (b)–(d) HRTEM and (e)–(h) EDAX mapping of the Pd-Ag (0.03) bimetallic NPs on the nylon nanofiber surface.

precursor concentration from 0.01–0.05 mM (figure S4) which was quantified through the ICP-MS measurements. Pd concentrations were nearly unchanged on all the bimetallic decorated nanofibrous webs which reveals the stable interaction of Pd on the polymer surface and stability during the chemical reduction based synthesis of the Ag-NPs. The ICP-MS analysis indicated the prepared Pd-Ag bimetallic NPs with the atomic ratios of $Pd_{40}Ag_{60}$, $Pd_{28}Ag_{72}$, and $Pd_{12}Ag_{88}$ were obtained when 0.01, 0.03, and 0.05 mM of $AgNO_3$ were used as a precursor, respectively. In the prepared monometallic and bimetallic nanofibrous webs, the Ag ions had a promising crystalline nature with the fcc phase as demonstrated by the XRD analysis (figure S5).

The broad diffraction peaks at 20.4° (100) and 23.0° (010, 110) represent the semicrystalline nature of the nylon nanofibrous webs. The presence of Pd was not detected by the XRD spectrum which may be due to the very low loading nature (nearly 3 wt% on the nanofiber surface) or may be due to the small size of the NPs, less than 2 nm which is non-detectable by XRD. For the bimetallic samples (111), the diffraction peaks were indeed between the Ag and Pd crystal structure which further confirms the bimetallic nature of the synthesized product. To investigate the electronic and structural effect on the bimetallic nanostructures, XPS spectra of the monometallic and different ratios of Pd-Ag bimetallic NPs in Pd 3d and Ag 3d were investigated. The high resolution peaks of Pd 3d and Ag 3d were deconvoluted into two pairs of doublets, as shown in figure 5.

A survey scan (figure S6) revealed the presence of Ag, Pd, O, C, and N in the samples. As in the monometallic phase of the Pd decorated nylon nanofibers, the comparative relative area of Pd^0 was higher than the Pd^{II} peaks, whereas upon decorating the Ag ions as the Pd-Ag-NPs this trend was maintained (figure 5(a)). This shows that the introduction of Ag ions neither increases the content of the Pd^{II} nor decreases
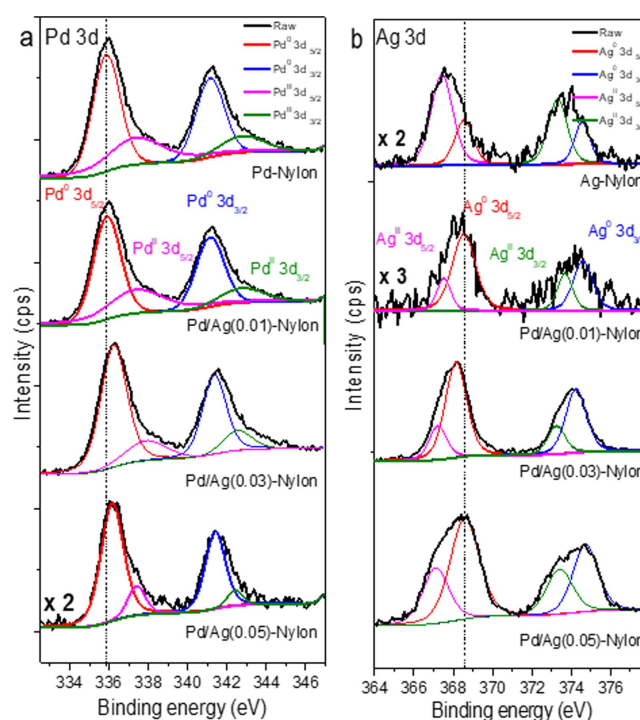

Figure 5. High resolution spectra of the Pd-Ag bimetallic nylon nanofibrous webs (a) Pd 3d and (b) Ag 3d.

the relative content of Pd^0 on the flexible nanofibrous web. The binding energy values of the Pd $3d_{5/2}$ and Pd $3d_{3/2}$ core level of the monometallic nanofibrous web appear at 335.9 and 341.2 eV, respectively.

But upon decorating the Ag ions on the Pd surface the core peak positions shifted due to the possible interaction between the bimetallic nanostructures. The possible shift in binding energy of Pd indicated the change in electronic states on the metallic NPs. The Ag 3d core level spectrum
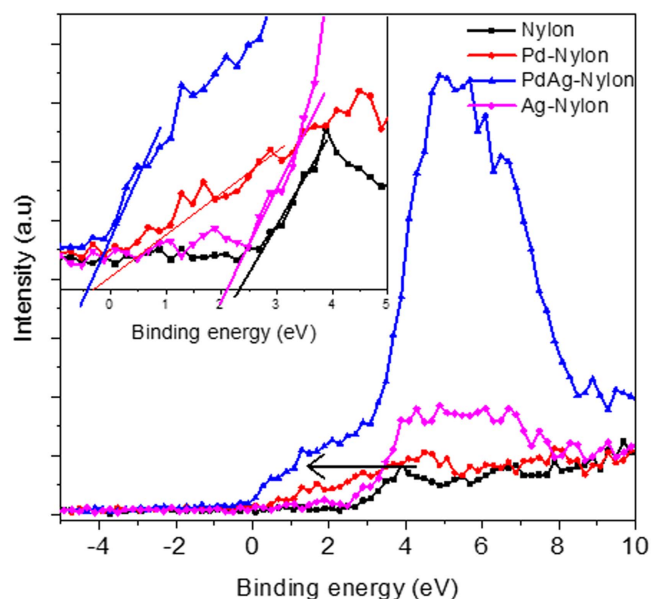
Figure 6. XPS VB spectra of the (a) nylon, (b) Pd-Nylon, (c) Ag-Nylon, and (d) Pd/Ag(0.03)-Nylon nanofibrous webs.

(figure 5(b)), exhibited two strong peaks at 367.6 and 373.7 eV, which were associated with Ag $3d_{5/2}$ and Ag $3d_{3/2}$, respectively, where in the bimetallic phase, the core level of the Ag ions was found to be constitutive primarily with the Ag^0, but after the chemical reduction of Ag ions with the monometallic nature on the nanofibrous web, the core level spectra primarily exhibited the Ag^{II} state. This observation state that in the bimetallic functionality of Ag and Pd ions were consistent with the XRD and TEM results. Though both metallic spectra have the existence of Ag^{II} and Pd^{II} states, it is interesting to understand the exact metallic nature of the nanofibrous web. As the XRD spectra do not show any evidence of metal oxide formation, the presence of Ag^{II} and Pd^{II} states from the XPS analysis demonstrates the oxidation of the catalyst surface in air. This may be due to the possibility of the chemisorption of a small amount of O_2 on the catalyst surface. It was also asymmetric towards the higher binding energy side. By observing the shift in the core level peak positions in the bimetallic samples when compared with the monometallic samples, it confirms the formation of a bimetallic nature [35–37] due to inter atomic charge redistribution caused by the valence band (VB) hybridization. The difference between the peak positions of $3d_{5/2}$ and $3d_{3/2}$ were absorbed to be 6.0 and 5.3 eV for the Ag and Pd, respectively which represented the zero valence state for all the bimetallic samples. The interaction of the metal–metal bond in the bimetallic NP form of nanostructures is favorable for the production of high binding energy density and enhancive catalytic properties [38]. The formation of Pd based bimetallic phases shifted the VB density for the production of excessive electrons which would later serve as a charge donor in catalytic reactions [39]. Besides understanding the shift in the core peak position of the bimetallic nanostructures, the change in the VB spectra of the bimetallic samples gives a clear

understanding of the bimetallic formation. Figure 6 shows the XPS VB spectra of the monometallic and bimetallic samples which have the broad peaks centered around 4 eV below the Fermi level. The spectral feature of the Pd-Ag bimetallic nanofibrous web have a broad shoulder at 2 eV with the tail at 0 eV.

The deconvolution of the peak into two was to clarify the contribution of the Ag and Pd to the bimetallic functionality. From the valence density of states (DOS) observation, the spectral difference reveals the direction of the valence charge polarization upon bimetallic formation. It evidences that charge migrated from the bottom to the upper edge of the VB in the Pd-Ag bimetallic NPs which is called charge polarization [40]. This effect shifts the valence DOS due to the polarization in Pd-Ag bimetallic NPs to generate excessive electrons at the upper edge which serve as charge donors in the catalytic process [40, 41]. The effective valence charge polarization effect differentiated the catalytic performance of the bimetallic NPs. The deconvoluted peaks were in good agreement with the Pd-Ag functionality as compared with the monometallic fibrous web. This shift denoted the possibility of the effective charge separation and electronic interaction between the Ag and Pd metal ions with bimetallic nature. As prepared Pd-Ag bimetallic NPs supported on a nylon nanofibrous web act as an effective catalyst in the hydrogenation process for the reduction of 4-NP to 4-AP.

Figure 7 shows the reduction of 4-NP in the Pd-Nylon, Pd/Ag(0.03)-Nylon, and Ag(0.03)-Nylon nanofibrous webs with respect to time. It could be seen that the catalytic reduction rate (figure 8) among the bimetallic nanofiber webs that the Pd/Ag(0.03)-Nylon nanofibrous web displayed higher catalytic activity with the competing time of 12 min for the complete reduction of 4-NP to 4-AP. Further, depending on the contribution of the Ag ratio to Pd on the polymeric web playing the key role in the catalytic reduction rate. Comparing the monometallic nanofibrous webs, the bimetallic loaded webs exhibited effective catalytic behavior, which displayed the existing effect between the Ag and Pd in the bimetallic form. The reduction rates of Pd/Ag(0.03)-Nylon ($0.152 \, min^{-1}$) were 5.85 and 3.16 times higher than the Ag-Nylon and Pd-Nylon nanofibrous webs. The higher catalytic activity from the Pd/Ag(0.03)-Nylon nanofibrous web were probably from the effective electron generation associated with the smaller dimension. Upon inducing the dosage variation of the Pd/Ag(0.03)-Nylon nanofibrous web, specifically at 0.5, 1, 2, and 4 mg of nanofibrous webs with the constant 4-NP concentration at $22 \pm 1\,°C$.

Figure 9(a) shows the catalytic reduction of 4-NP in the presence of different dosages of Pd/Ag(0.03)-Nylon nanofibrous webs. Upon increasing the dosage, the reduction rate increased linearly. The insert shows that the reduction rate kinetics increased linearly with the catalyst dosage. The linear behavior indicated the reduction rate in the first order kinetic with respect to the concentration or dosage of the Pd/Ag(0.03) nanostructures. In order to understand the activation energy of 4-NP by the bimetallic
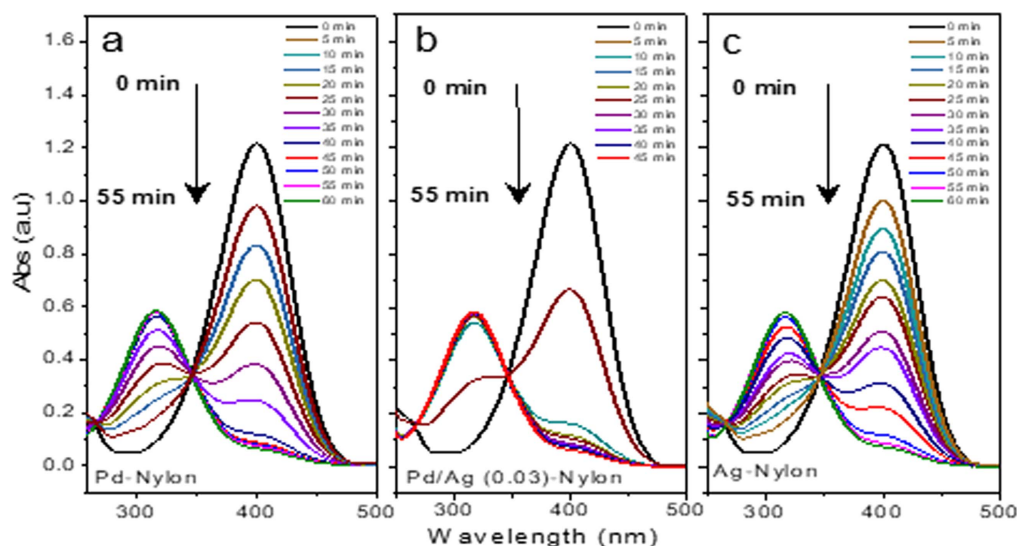
Figure 7. UV–vis absorption over the 4-NP reduction with respect to time with catalyst webs (a) Pd-Nylon, (b) Pd/Ag(0.03)-Nylon, and (c) Ag-Nylon.

NPs, the reaction was initiated under different temperatures ranging from 12 °C–42 °C. From the rate constant value under different temperatures, the values of the Arrhenius plot (i.e., ln *k* versus 1/T) were drawn and the apparent activation energy was calculated (3.053 kJ mol^{-1}) [42]. While decorating the Ag ions without the Pd-NPs on the nylon nanofiber surface, they cannot favor the interaction on the nanofiber surface and exhibited the Ag^{II} state. This phenomenon indicated the facilitated reduction of Ag ions on the Pd surface by acting as nuclei in the chemical reduction process during the formation of the bimetallic NPs. Providing the Pd as a nucleation site for the Ag favors the effective synthesis process for the formation of Pd-Ag bimetallic nanostructures with different atomic ratios by controlling the precursor concentration and ALD cycles.

In the catalytic process, Pd-Ag bimetallic NPs on the nylon nanofibrous web exhibited enhanced catalytic activity and durability. The turnover frequency (TOF) values (table 1) manifests the effective role of Ag as a bimetallic form of catalyst and promotes its catalytic efficiency. The shift in the binding energy on the Pd-Ag bimetallic NPs demonstrates the enhanced electron density of Pd-NPs by alloying with Ag ions, which may be due to the donation of electrons from the Pd atom to the π orbital of the intermediates. The favorable higher production rate of electrons increases the bonding strength of reactive species on the Pd surface and enhances the reaction kinetic. The reusable properties of the bimetallic NP decorated nylon nanofibrous web based catalyst were investigated up to five cycles. After each cycle the catalytic web transferred into 0.1 mM of fresh 4-NP solution with constant shaking at 320 rpm. As shown in figure 10, 4-NP was reduced by the Pd/Ag(0.03)-Nylon nanofibrous web at five cycles under the ambient condition. The catalytic activity reduced with the number of cycles and the reduction rate decreased from 0.158–0.0345 min^{-1} after five cycles. Over the reusable cycles the conventional time for the complete degradation of the catalytic reaction was increased due to the surface oxidization functionality. In this observation, the
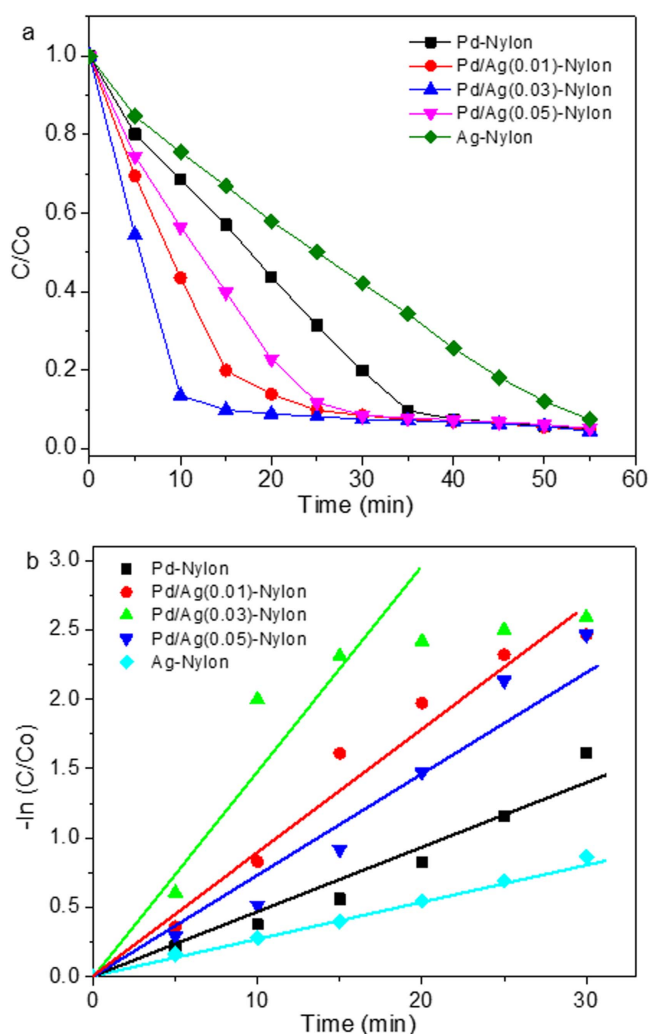

Figure 8. (a) Catalytic reduction and (b) kinetic rate of the 4-NP reduction with respect to time with the catalyst web.

bimetallic nanofibrous web exhibited more stable reusable catalytic behavior as compared with the monometallic nanofibrous webs. After two consecutive catalytic cycles the
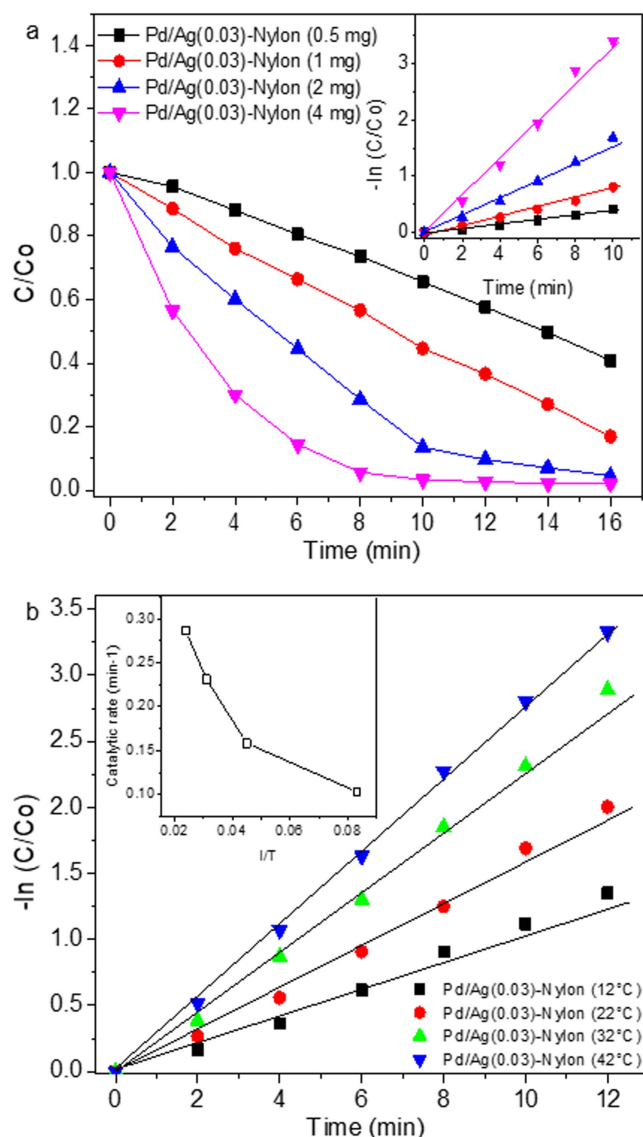
Figure 9. (a) Plot of reaction time versus catalytic reduction rate of 4-NP catalyzed by various dosages of the Pd/Ag(0.03)-Nylon nanofibrous web. The inset shows a plot of the natural logarithm of the reduction rate versus the catalyst concentration (rate $= \min^{-1}$; [4-NP] $= 0.1$ mM, $T = 22$ °C ± 1 °C). (b) Plot of reaction time versus catalytic reduction rate of 4-NP catalyzed by the Pd/Ag (0.03)-Nylon nanofibrous web at various temperatures. The inset shows the Arrhenius plot, i.e., a plot of ln k versus $1/T$ ([4-NP] $= 0.1$ mM, [Pd/Ag-Nylon] $= 1$ mg).

Ag decorated nylon nanofibrous web did not exhibit any catalytic behaviors, which may be due to the poor interaction of the Ag ions with the polymeric surface which released or detached from the web finished in the first two cycles. Thus, the nanofibrous web did not participate in the multiple reusable catalytic processes. But the leaching of Pd and Pd-Ag bimetallic ions was minimal due to the strong interaction of the Pd-polymer interface through the ALD process.

The SEM images of the catalytically reused Pd/Ag (0.03)-Nylon nanofibrous web do not show any notable change, so the decrease in the catalytic activity of the Pd/Ag (0.03)-Nylon nanofibrous web may be due to the loss of the
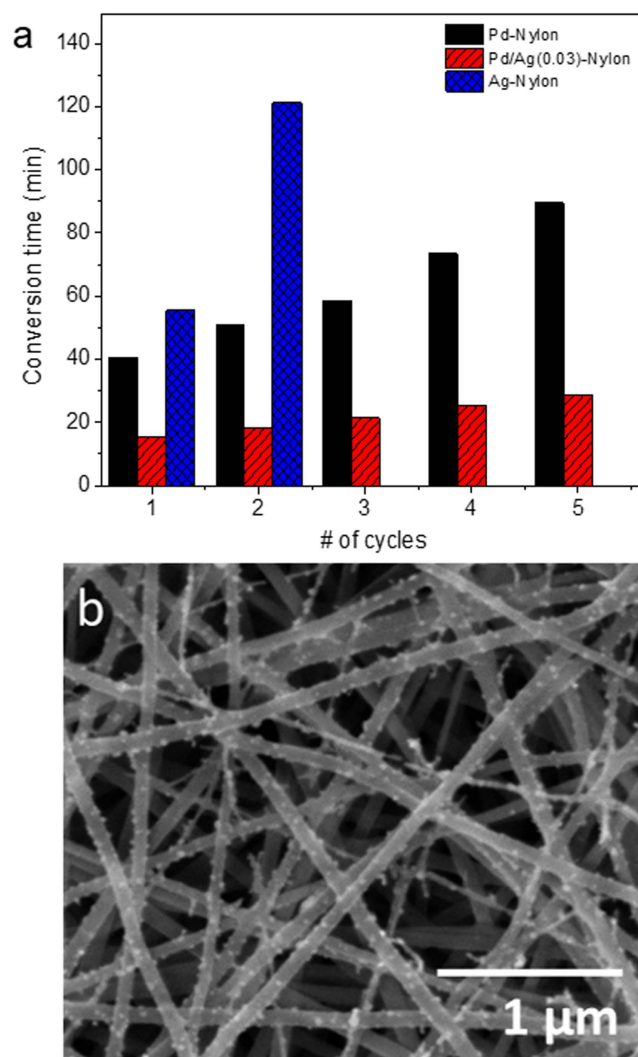

Figure 10. (a) Reusable properties and (b) structural stability of the bimetallic loaded nylon nanofibrous web (Pd/Ag (0.03)-Nylon).

metal ions from the nanofibrous web or the deactivation effect caused by the oxidation of the metal nature during the reduction of 4-NP. After the catalytic process, XPS analysis showed that the Pd 3d peaks of the reused catalyst shift to lower binding energy compared with the fresh one (figure S7), which may be due to the oxidization nature of the catalyst. This results in the shift in binding energy. The presence of a small amount of Ag ions after the catalytic process in the supernatant liquid was confirmed by the ICP-MS that revealed the leaching of the catalyst during the catalytic reaction which is the key to the catalytic deactivation in multiple cycles.

Catalytic mechanism

The mechanism behind the effective improvements or enhancements of the heterogeneous catalytic activity of the Pd loaded polymeric web with the Ag functionality is proposed in figure 11. As from the previous investigations the catalytic reduction of the NPs were governed by the interaction of BH_4^- on the catalytic surface with the promoted

Table 1. Comparison of the reduction of 4-NP with different catalysts.

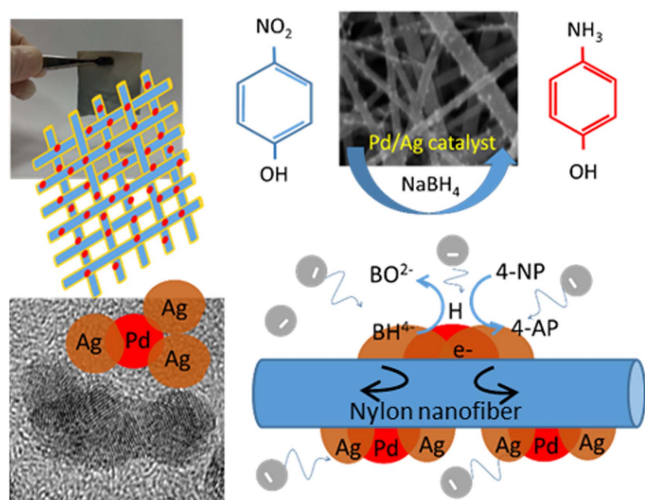| Catalyst	Mass of the catalyst (mg)	Amount of 4-NP (mM)	Amount of NaBH$_4$ (mM)	Metal size (nm)	Metal contents (wt%)	Conversion time (min)	TOF	Reference
Pd-Nylon	2	1×10^{-1}	7	2	2.7	35	0.055	Present work
Pd/Ag (0.03)-Nylon	2	1×10^{-1}	7	2–5	7.6	12	0.138	Present work
Au/graphene	0.1	2.8×10^{-4}	2×10^{-2}	14.6	24	12	0.19	[45]
Au@C	5	3×10^{-4}	3×10^{-2}	15	NA	5		[46]
Ag/carbon	1	3.6×10^{-3}	15×10^{-2}	28.1	8.4	8	0.58	[47]

Figure 11. A possible schematic mechanism for the catalytic reduction of a 4-NP by Pd/Ag-Nylon nanofibrous web.

absorption rate of reactants and effective hydrogen transfer to the 4-NP through the metal catalyst [42, 43]. The loading of Pd metal ions on the polymeric web induces the strong metal support interaction which manifests the favorable electron transfer. The effective substitutional effect of Ag modifies the electron density in the bimetallic surface which improves the electron density. The favorable modifications were led by the effective loading ratio of Ag which favors electron deficiency or electrophilicity [44]. The favorable formation of 4-nitrophenolate ions was because of the BH_4^- ions being preferably attracted by the bimetallic surface due to its negatively charged nature, which is believed to be in accordance with the Langmiur–Hinhelwood mechanism [43]. On the other hand, BH_4^- ions could possibly donate electrons to the electron deficient bimetallic surfaces and this leads to the production hydrogen atoms by the cleavage of the B–H bond over the Pd-Ag catalyst. The produced hydrogen ions are thermodynamically unstable and favorable for the interaction with 4-nitrophenolate ions through the conventional hydrogenation route. The reaction rate on the catalytic surface mainly depends on the electron density on the bimetallic surface which has been decided by the ratio difference of the bimetallic functionality. This leads to the reduction effect on the catalytic reaction towards the flexible bimetallic nanofibrous web.

Conclusions

In summary, we designed a Pd-Ag based bimetallic nanoparticles on a nylon nanofibrous web fabricated by combining electrospinning followed by ALD with the combination of a chemical reduction process. Decorating the ultra-sized Pd-NPs with the size of ∼2 nm initiated the nucleation of Ag on its surface to form the bimetallic NPs. The slow interaction leads to the consequent loading of Ag ions on the Pd surface which lead to the formation of Pd-Ag bimetallic NPs. The constructed bimetallic particles were notable for their

effective reduction of 4-NP with a durable and easily recoverable nature. The ratio of Ag on the Pd surface shows that the compositional form of the bimetallic face plays a critical role in effective catalytic behavior. The synergistic effect between Ag and Pd leads to a change in its electronic nature which favors the improved catalytic activity. The nanofibers exhibited first order catalytic kinetic behavior with respect to the catalytic dosage and the activation energy of the catalyst was determined to be 3.053 kJ mol^{-1}. Nearly 92% of the initial bimetallic catalytic activity remained in time even after five cycles and the nanofibrous web were more stable even after the multiple catalytic reductions. Through the exhibition of tunable functionality over the catalytic behavior of Pd-Ag bimetallic particles, its great potential in a vast number of multifunctional applications has to be explored.

ORCID iDs

Tamer Uyar ⓘ https://orcid.org/0000-0002-3989-4481

References

[1] Pascanu V, Gomez A B, Ayats C, Prats A E P, Carson F, Su J, Yao Q, Pericas M A, Zou X and Matute B M 2015 *ACS Catal.* **5** 472–9
[2] Li X, Guo Z, Xiao C, Goh T W, Tesfagaber D and Huang W 2014 *ACS Catal.* **4** 3490–7
[3] Li X, Goh T W, Li L, Xiao C, Guo Z, Zeng X C and Huang W 2016 *ACS Catal.* **6** 3461–8
[4] Ganapathy D and Sekar G 2014 *Org. Lett.* **16** 3856–9
[5] Sun W, Yang W, Xu Z, Li Q and Shang J K 2016 *ACS Appl. Mater. Interfaces* **8** 2035–47
[6] Xu Z N, Sun J, Lin C S, Jiang X M, Chen Q S, Peng S Y, Wang M S and Guo G C 2013 *ACS Catal.* **3** 118–22
[7] Pacardo D B, Sethi M, Jones S E, Naik R R and Knecht M R 2009 *ACS Nano* **3** 1288–96
[8] Wang L, Dong Y, Zhang Y, Zhang Z, Chi K, Yuan H, Zhao A, Ren J, Xiao F and Wang S 2016 *NPG Asia Mater.* **8** e337
[9] Maiti P S, Houben L and Sadan M B 2015 *J. Phys. Chem. C* **119** 10734–9
[10] Yamamoto K, Imaoka T, Chun W J, Enoki O, Katoh H, Takenaga M and Sonoi A 2009 *Nat. Chem.* **1** 397–402
[11] Tian N, Zhou Z Y, Sun S G, Ding Y and Wang Z L 2007 *Science* **316** 732–5
[12] Lim B, Jiang M, Camargo P H, Cho E C, Tao J, Lu X, Zhu Y and Xia Y 2009 *Science* **324** 1302–5
[13] Jiang X, Koizumi N, Guo X and Song C 2015 *Appl. Catal. B* **170–171** 173–85 2015
[14] Zhang L, Su H, Sun M, Wang Y, Wu W, Yu T and Zeng J 2015 *Nano Res.* **8** 2415–30

[15] Bondarchuk I S and Mamontov G V 2015 *Kinet. Catal.* **56** 379–85

[16] Imura Y, Tsujimoto K, Morita C and Kawai T 2014 *Langmuir* **30** 5026–30

[17] Huang J, Vongehr S, Tang S, Lu H and Meng X 2010 *J. Phys. Chem.* C **114** 15005–10

[18] Ma Q, Sun J, Gao X, Zhang J, Zhao T, Yoneyama Y and Tsubaki N 2016 *Catal. Sci. Technol.* **6** 6542–50

[19] De Corte S, Hennebel T, Fitts J P, Sabbe T, Bliznuk V, Verschuere S, van der Lelie D, Verstraete W and Boon N 2011 *Environ. Sci. Technol.* **45** 8506–13

[20] Hang L, Zhao Y, Zhang H, Liu G, Cai W, Li Y and Qu L 2016 *Acta Mater.* **105** 59–67

[21] Yin Z, Zhang Y, Chen K, Li J, Li W, Tang P, Zhao H, Zhu Q, Bao X and Ma D 2014 *Sci. Rep.* **4** 4288

[22] Sankar M, Dimitratos N, Miedziak P J, Wells P P, Kielye C J and Hutchings G J 2012 *Chem. Soc. Rev.* **41** 8099–139

[23] Convertino A, Cuscuna M, Martelli F, Manera M G and Rella R 2014 *J. Phys. Chem.* C **118** 685–90

[24] Sai V V R, Gangadean D, Niraula I, Jabal J M F, Corti G, McIlroy D N, Aston D E, Branen J R and Hrdlicka P J 2011 *J. Phys. Chem.* C **115** 453–9

[25] Lee J S, Kwon O S, Park S J, Park E Y, You S A, Yoon H and Jang J 2011 *ACS Nano* **5** 7992–8001

[26] Wang Y, Qu Q, Han Y, Gao T, Shao J, Zuo Z, Liu W, Shi Q and Zheng H 2016 *J. Mater. Chem.* A **4** 10314–20

[27] George S M 2010 *Chem. Rev.* **110** 111–31

[28] Ranjith K S, Celebioglu A, Eren H, Biyikli N and Uyar T 2017 *Adv. Mater. Interfaces* **4** 1700640

[29] Khaliy M A, Eren H, Albayrah S, Sasapto H H, Biyikli N, Ozkar S and Guler M O 2016 *Angew. Chem. Int. Ed.* **55** 12257-61

[30] Jing H and Wang H 2015 *Chem. Mater.* **27** 2172–80

[31] Fatma K, Akgun C O, Donmez I, Biyikli N and Uyar T 2012 *ACS Appl. Mater. Interfaces* **4** 6185–94

[32] Li Z, Huimin H, Shang T, Yang F, Zheng W, Wang C and Manohar S K 2006 *Nanotechnology* **17** 917–20

[33] Formo E, Yavuz M S, Lee E P, Lane L and Xia Y 2009 *J. Mater. Chem.* **19** 3878–82

[34] Navaladian S, Viswanathan B, Varadarajan T K and Viswanath R P 2009 *Nanoscale Res. Lett.* **4** 471–9

[35] Abrikosov I, Olovsson W and Johansson B 2001 *Phys. Rev. Lett.* **87** 176403

[36] Ji W, Zhang C, Li F, Li P, Wang P, Ren M and Yuan M 2014 *RSC Adv.* **4** 55781–9

[37] Liu M, Chi F, Liu J, Song Y and Wang F 2016 *RSC Adv.* **6** 62327–35

[38] Rodriguez J A and Goodman D W 1992 *Science* **257** 897–903

[39] Ontaneda J, Bennett R A and Crespo R G 2015 *J. Phys. Chem.* C **119** 23436–44

[40] Sun C Q 2010 *Nanoscale* **2** 1930–61

[41] Liu X *et al* 2015 *Chem. Rev.* **115** 6746–810

[42] Roduner E 2014 *Chem. Soc. Rev.* **43** 8226–39

[43] Wunder S, Lu Y, Albrecht M and Ballauff M 2011 *ACS Catal.* **1** 908–16

[44] Pozun Z D, Rodenbusch S E, Keller E, Tran K, Tang W J, Stevenson K J and Henkelman G 2013 *J. Phys. Chem.* C **117** 7598–604

[45] Li J, Liu C Y and Liu Y 2012 *J. Mater. Chem.* **22** 8426–30

[46] Liu R, Mahurin S M, Li C, Unocic R R, Idrobo J C, Gao H, Pennycook S J and Dai S 2011 *Angew. Chem. Int. Ed.* **50** 6799–802

[47] Zhang P, Shao C, Zhang Z, Zhang M, Mu J, Guo Z and Liu Y 2011 *Nanoscale* **3** 3357–63